Spring 5-20-2021

# Development and Implementation of a Pressure-Temperature Control System for the Physical Vapor Deposition of Copper and Niobium from a Molybdenum Filament in the Development of Superconducting 3D Printed RF Cavity Particle Accelerators

Chandler J. Fleuette
*University of New Hampshire, Durham*

# Development and Implementation of a Pressure-Temperature Control System for the Physical Vapor Deposition of Copper and Niobium from a Molybdenum Filament in the Development of Superconducting 3D Printed RF Cavity Particle Accelerators

Chandler Fleuette*
*University of New Hampshire: Long Lab, Durham, NH, 03824, USA*
(Dated: May 20, 2021)

This report covers the development of the pressure-temperature control system used in the production of small superconducting RF cavities for particle accelerators. To test the validity of the created program, a model for the process was created and tested. The model was used to fine tune the control system before integrating it into the lab. The end goal of the control system is to measure the pressure inside of a deposition vacuum chamber, convert that pressure to a temperature, and use that temperature in tandem with a PID controller to control the current passing though a molybdenum filament which is used as the carrier mechanism for a copper thin film coating in a physical vapor depositing (PVD) process.

The basis for this project comes from creating 3D-printed RF cavities that will be coated in a superconducting material. In being able to produce multiple units of these cavities, it is possible to string together multiple units to create an in-house particle accelerator. A cross section of a single unit can be seen in Fig. (1).

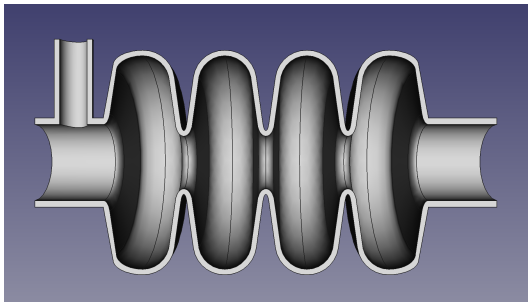

Figure 1: CAD RF cavity cross section.

To make the cavities, multiple steps need to be addressed, from the 3D-printing of the cavity as one piece for a smooth thin film coating on the interior of the cavity, to the control of the deposition rate of the thin film coating. A superconducting thin film coating is radially deposited onto the interior of the RF cavity structures. This structure is specifically designed to be easily reproducible using table-top 3D printing.

To make the structure superconducting, a superconducting material is deposited on to the structure using Physical Vapor Deposition (PVD). The superconducting material chosen for the end product is niobium (Nb). To test initial viability, copper is currently being used as a stepping stone to see if a conducting RF cavity is possible.

PVD is the process in which a condensed matter phase, either solid or liquid, is vaporized and deposited onto a substrate. After thermal vapor deposition, where the deposition material is vaporized, the material condenses on the substrate in such a way that a condensed solid phase is formed [1].

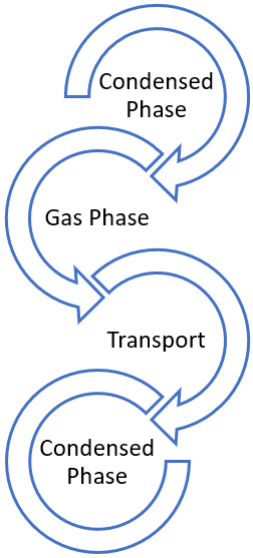


Figure 2: Physical Vapor Deposition Overview Cartoon

The cartoon graphic seen in Fig. (2) helps to outline the PVD process, from starting in a condensed phase, transitioning to a gas phase for transport to the deposition surface, where the material condenses back into a solid phase. Ideally, an equilibrium vapor pressure is found during PVD, in which there is no transfer of material from one state to the other. This pressure is tied to a specific temperature, or more realistically, a function that is dependent only on temperature [1].

Due to the material considerations for this experiment, the carrier filament used must be molybdenum (Mo). Normally a tungsten filament would be used as the carrier, but because tungsten chemically attacks niobium, the superconducting properties of the deposited material are lost. When switching to molybdenum as the filament, temperature control becomes a much greater issue. This is because of how close the vaporization point tempera-

ture of molybdenum and niobium are to one another.

Molybdenum has a vaporization point of 2623[°C] and niobium's vaporization point is 2477[°C]. Having vaporization temperatures so close to one another mean that a sensitive temperature control system needs to be developed. If the molybdenum filament begins to melt and is deposited on to the interior surface of the RF cavity during the deposition of niobium, the superconductivity of the deposition layer will be compromised.

The goal of the control system is to maintain a set-point temperature inside a vacuum chamber during physical vapor deposition. Directly measuring the pressure inside the vacuum chamber allows for a temperature value to be calculated. The temperature calculated from the pressure would then be used to correct the current output from the connected power supply. This would increase or decrease the pressure inside the vacuum chamber such that the equilibrium temperature inside the chamber is equivalent to the vaporization temperature of the deposition material.

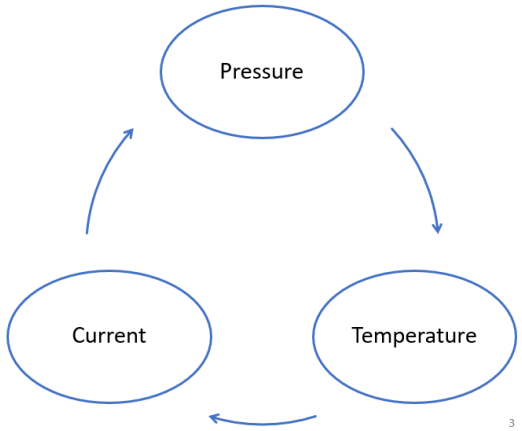


Figure 3: Control system overview, where starting with the pressure, a temperature is calculate and a current value is found. This current either increases or decreases the pressure inside the chamber resulting in a new temperature value, repeating the cycle.

Figure (3) is a handy graphic for visualizing the control process. Where the initial pressure inside the vacuum chamber is measured, which is converted to a temperature. This temperature is compared to the set-point temperature of the system and the current passing through the Mo filament is adjusted such that the pressure inside the chamber adjusts accordingly.

As access to the lab was limited due to the ongoing COVID-19 pandemic, a computer model was developed in LabVIEW to verify the control system. This would streamline the implementation of the control system in the lab and also act as a sanity check to see if such a system was possible.

The starting point of the model was to take the pressure-temperature relation provided by [2],

$$\log(P) = A + \frac{B}{T} + C\log(T) + D \cdot T \cdot 10^{-3}. \quad (1)$$

In the equation the parameters $A$, $B$, $C$, and, $D$ are constants determined "for the 65 metallic elements up to and including curium."[2]. Eq. (1) is considered the "precise" equation for determining the pressure from a given temperature for specific metallic elements, as it returns values for the log of $P$ to $\pm 1\%$. Here the pressure, $P$, is in units of Atmospheres and the temperature, $T$, is in units of Celsius. It is important to note that the vacuum gauge controller in the lab outputs pressure values in units of Torr, so an additional conversion, $P_{atm} = \frac{P_{Torr}}{760}$, needs to be done. The logarithm in Eq. (1) is also a log base 10 ($\log_{10}$) and not a natural log (ln).

However, using the "precise" equation, where the parameter $D$ is non-zero, makes the maths for find temperature as a function of pressure extremely complex and impossible to compute analytically. As such, having a lower order equation makes solving for temperature possible analytically. In Alcock, et.al. [2], a "practical" equation is presented as

$$\log P = A + \frac{B}{T} + C\log(T). \quad (2)$$

Reducing Eq. (1) down to a two-term equation produces unrealistic and unacceptable results for the majority of metallic elements. This leaves only the three-term "practical" equation, Eq. (2), where $D = 0$, for use in the control system which returns a value for the log of pressure to $\pm 5\%$.

Eq. (2) can be solved analytically. Using MatLab a parameterized equation for temperature as a function of pressure was found;

$$T(P) = -\Re\left[\frac{B}{C \times \omega_W\left(\frac{-\log\left(\frac{-C}{B}\right)-(-\log(P)-A\log(10))}{C\log(10)}\right)}\right]. \quad (3)$$

Where the Wright Omega function,

$$\omega_W(x) = W_{\lceil \frac{\Im(x)-\pi}{2\pi} \rceil}(e^x). \quad (4)$$

is found in the denominator and is defined as seen in Eq. (4). Here the Wright Omega function is defined in terms of the Lambert W function, $W_k(z)$, otherwise known as the omega function. The Wright Omega function is a resolution to the equation $z = \ln(z)$ and also satisfies the relation $W_k(z) = \omega(\ln(z) + 2\pi ik)$.

By taking the real part of the value calculated from Eq. (3), the temperature for any metallic element at any

pressure can be found. Refer to [2] for a comprehensive list of material parameters. With the parameterized analytical solution to the pressure-temperature relation found, a basic model for the relation between current and pressure was found using data points from previous deposition runs.

$$P = I \cdot 1^{-5} - 9^{-6} \tag{5}$$

| Current — [A] | Pressure — [Torr] |
|---|---|
| 3.50 | 3.60E-05 |
| 3.80 | 4.80E-05 |
| 4.00 | 5.10E-05 |
| 4.20 | 5.50E-05 |
| 4.90 | 6.10E-05 |
| 5.30 | 6.70E-05 |
| 5.60 | 7.10E-05 |

Table I: Data collected from previous deposition runs to determine the current-pressure relation.

The basic current pressure relation found is Eq. (5), and the data-points used are listed in Table I.

To round out the calculation process inside the model, a time-dependent factor was added. The motivation for this being that when the current is changed, the temperature is not instantaneously changed as well in a physical system. There is a time gap in real-world conditions, which,

$$T = T_0 \left(1 - e^{-ct}\right), \tag{6}$$

corrects for. The physical parameter $c$ in Eq. (6) was found to be 1.72 for the system. This gives the "time constant" for the system, $\tau$, as $\frac{1}{c} = 0.581\,[s]$.

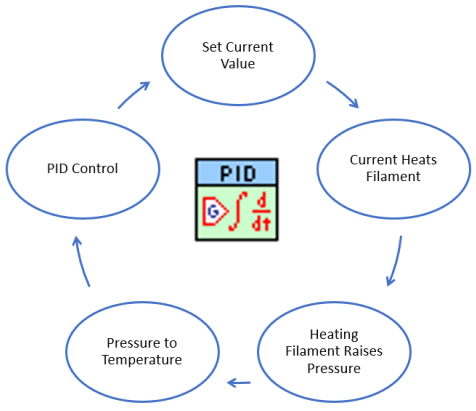


Figure 4: Cartoon of LabVIEW control system. An arbitrary current is set, which would heat a filament setting a pressure value. This value is converted to temperature using Eq. (3), which is passed into a PID controller. The PID outputs a value for the current such that the process variable, temperature calculated from pressure, reaches the set-point temperature.

Figure (4) outlines the model control system. With the basic conversion for current to pressure, the "practical" equation for temperature, and the associated system temperature delay consideration, the monitored temperature is passed into a Proportional Integral Derivative (PID) autotuning controller. The PID controller takes in a set-point, $(SP)$, in this case the vaporization temperature of the deposition material and the process variable, $(PV)$, the temperature calculated from the pressure.

The controller then outputs a value for the current which changes the process temperature such that it approaches the vaporization temperature. To make this correction, the PID computes three different parameters: the proportional, integral, and derivative responses.

The proportional component, referred to as the Error term, is simply the difference between the set-point value (vaporization temperature) and the process variable (temperature in the vacuum chamber) [3][4]. The integral component sums the Error term over time. The purpose of the integral component is to drive the final Error term, Steady-State Error, to zero [3][4]. While the Error term is not zero, the integral component will increase continuously over time [3][4]. Finally the derivative component is used to decrease the output of the PID if the process variable is rapidly increasing [3][4]. This component is proportional to the rate of change of the process variable. The derivative component is also extremely sensitive to noise in the process variable signal, so for practical purposes the derivative time $(T_d)$ is small [3][4].

The proportional,

$$u_p(t) = K_c \mathcal{E} = K_c \left(SP - PV\right), \tag{7}$$

integral,

$$u_I(t) = \frac{K_c}{T_i} \int_0^t \mathcal{E} dt, \tag{8}$$

and derivative,

$$u_D(t) = K_c T_d \frac{d\mathcal{E}}{dt}, \tag{9}$$

actions are defined by Eq. (7), (8), and (9) respectively as outlined in [3]. Combining these formulas gives the calculation performed by a PID controller,

$$u(t) = K_c \left[\mathcal{E} + \frac{1}{T_i} \int_0^t \mathcal{E} dt + T_d \frac{d\mathcal{E}}{dt}\right]. \tag{10}$$

Where $K_c$ is the controller gain.

The PID needed to be autotuned so that the proportional gain, $K_c$, integral time, $T_i$, and derivative time, $T_d$ are optimized for each material that the control system will work for. LabVIEW has a autotuning PID controller that will automatically autotune the controller.

As a general rule, proportional gain is the largest PID parameter, followed up by integral time, with the derivative time minimized to prevent the PID from not approaching the set-point value. Once appropriate gains where found, a button was added to the model so that whenever the set-point temperature was updated, the PID would begin to correct for the new set-point temperature. Lastly, the wanted values from the process i.e. Process Temperature, Set-Point Temperature, Pressure, Current, Time and in the finalized control system, Voltage, were exported and appended into a lvm file so that analysis of the process could be done.

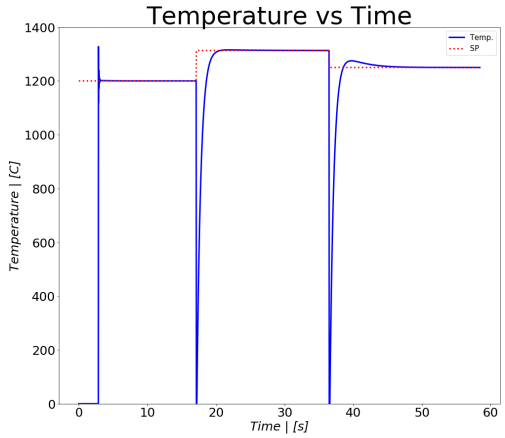


Figure 5: Temperature vs Time from Model data in blue with the set-point temperature as the dotted red line.

Fig. (5) is the model data for Temperature vs Time. Followed by Figure (6) a Current vs Time plot for the model date. Pressure vs time is not shown, as the pressure plot follows the same structure of the Temperature vs Time plot.

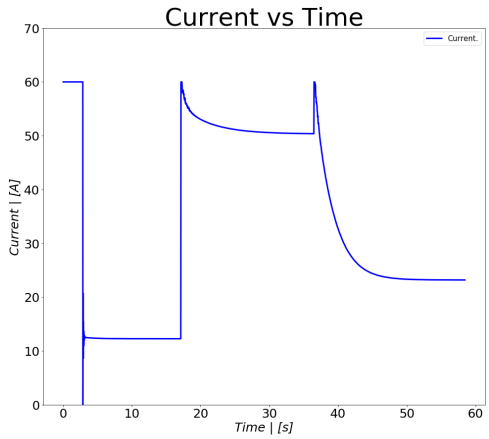


Figure 6: Current vs Time from Model data in blue. When the set-point temperature changes the current is set to a maximum.

As Fig. (5) shows, the PID sets the temperature to the desired set-point temperature. The model does have some difficulty dealing with changes to the set-point temperature or when initiating a temperature. The issue can be found in Fig. (6). When the set-point is initiated, the temperature drops to its minimum before settling into the set-point temperature, and likewise, the current instantaneously jumps to its maximum allowed output before settling into its steady-state. For every change to the set-point after the initial, the current and temperature jump to a minimum or maximum respectively, before approaching the steady-state value. This is an issue within the constructed model which for practical purposes can be ignored, as the lab data will show.

When doing deposition runs in the lab, copper (Cu) was used as the deposition material so that there was a large gap in vaporization temperatures between the carrier filament (Mo) and deposition material.

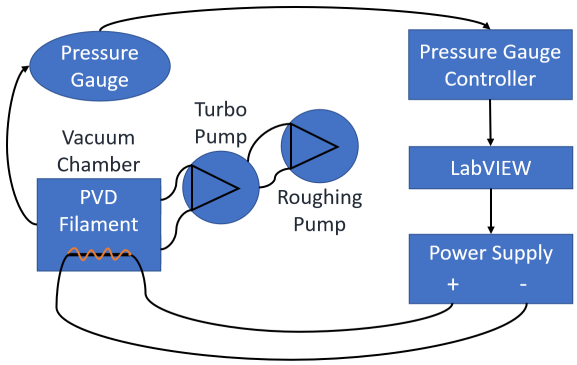


Figure 7: Schematic of the: pressure gauge controller, LabVIEW (computer), power supply, vacuum chamber, turbo and roughing pumps, and pressure gauge, in the Long Lab.

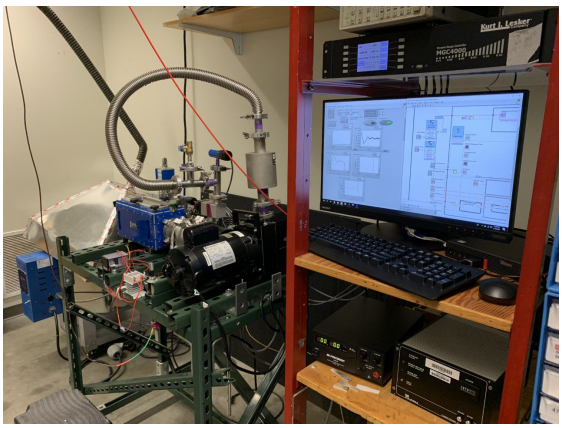

Figure 8: Physical Lab setup in the Long lab at the University of New Hampshire.

Figure (7) is a cartoon schematic of the lab setup in the Long lab at the University of New Hampshire. In the lab, LabVIEW (computer) is connected via a USB connection

to the power supply, which controls the current through the PVD filament. The vacuum chamber is connected to both a pressure gauge and a turbo pump, where the turbo pump is connected to a roughing pump. The turbo and roughing pumps are used to evacuate the vacuum chamber so that the low pressures required during PVD can be reached. From there, the pressure gauge outputs the pressure inside the vacuum chamber to the pressure gauge controller which then feeds the pressure value to the LabVIEW program in the computer via an RS232 connection. Figure (8) is a picture taken in the lab which shows the full physical lab setup as depicted by Fig. (7).

The front panel (user interface), Fig. (9), of the LabVIEW program was constructed such that realtime plots for the current, voltage, pressure, and temperature vs time could be seen simultaneously. There are multiple buttons present, one to set the set-point temperature to zero, one for resetting the time, which was read in seconds. This button was redundant, but adds a functionallity to the program so that a user can reset the time i.e. $t = 0[s]$ during operation.

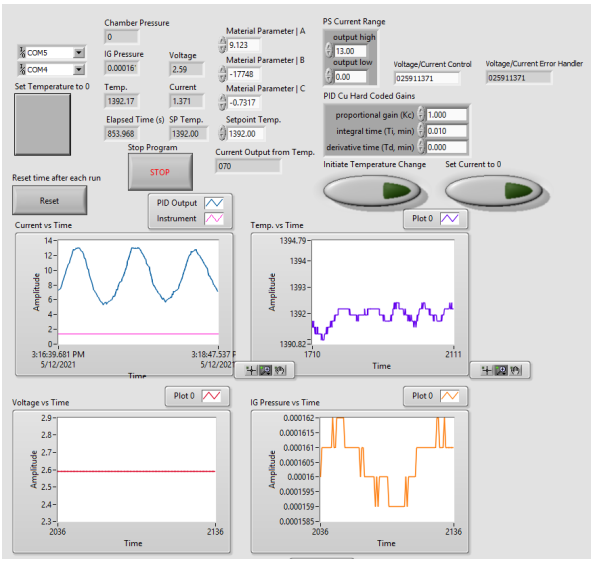


Figure 9: LabVIEW front panel (user interface) during a deposition run. As seen by the current and temperature plots the system is in a steady-state oscillation.

Other buttons present on the interface are the "Initiate Temperature Change" button, which is pressed whenever a new set-point temperature is input into the system and is wanted to be set by the operator. Lastly there is a button that sets the current output by the power supply to zero. This is present for safety reasons.

During trial runs of the control system, temperature control was achieved. This was done multiple times at different set-point temperatures to validate that the system was working correctly.

As Figures (10) and (11) show, steady-state oscillations were achieved in both temperature and current respectively. For temperature specifically, it is shown that different set-point temperatures can be reached and controlled to $\pm 1[^{\circ}\mathrm{C}]$. The period of oscillation in current, which controls the steady-state oscillation in temperature, can be shortened, along with the amplitude of oscillation, by better PID gain values. With better gain values, the data collected in lab will begin to look more like that of the ideal control system presented by the pressure-temperature model outlined above.

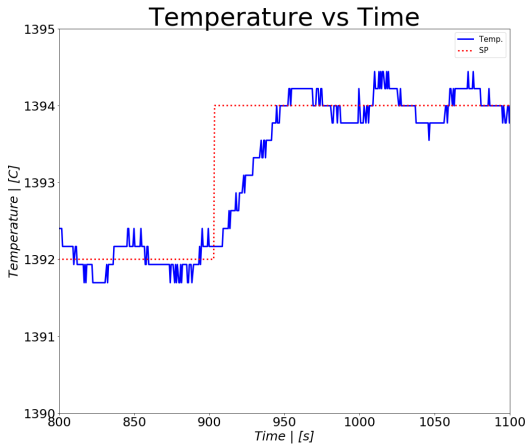


Figure 10: Proof of steady-state oscillations in temperature about the set-point temperature to $\pm 0.5[^{\circ}\mathrm{C}]$.

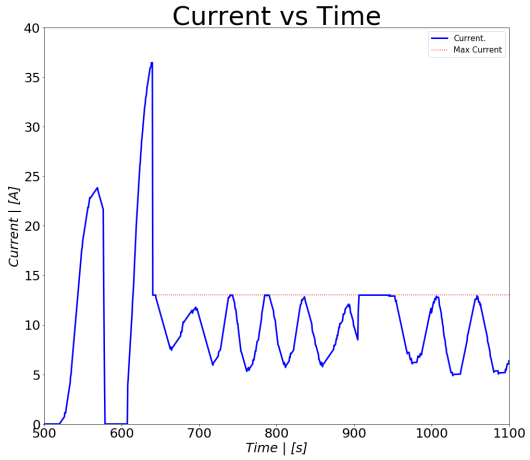


Figure 11: Proof of steady-state oscillations in current for temperature control

Two deposition runs were attempted. In one the pressure-temperature control system did not function properly, resulting in the power supply spiking to a maximum current to increase the pressure inside the vacuum chamber as fast as possible. The issue with this was that the quick increase in current did not increase pressure or temperature as the current passing through the molybdenum filament was great enough to fully melt it. This re-

sulted in an uncontrolled bombardment deposition which gave a poor thin film layer shown in Figure (12b).

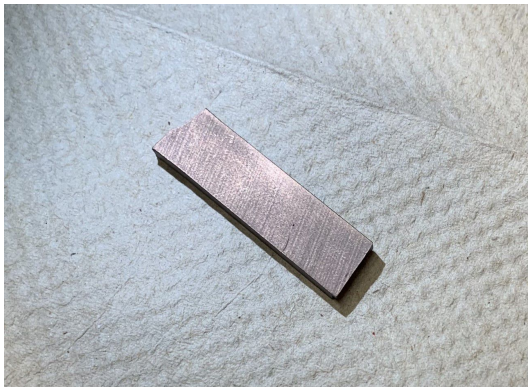

(a) Thin film coating of copper (Cu) during a deposition where the pressure-temperature control system worked in controlling the set-point temperature.

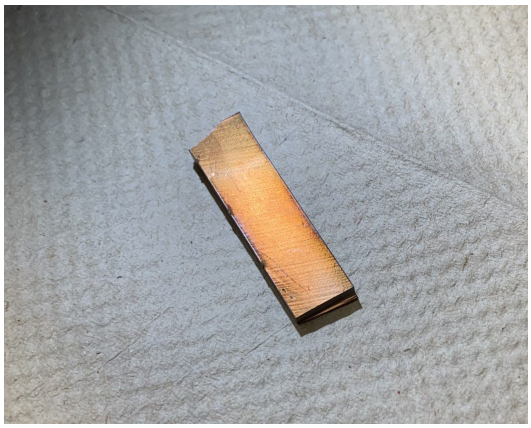

(b) Thin film coating of copper (Cu) during a deposition where the pressure-temperature control system malfunctioned and output maximum current through the molybdenum (Mo) filament, resulting in an uncontrolled bombardment deposition.

Figure 12: Copper (Cu) deposition results with and without the pressure-temperature control system working.

During the controlled deposition run, which resulted in the smoother thin film coating shown in Figure (12a), a vaporization temperature was set as the set-point temperature of the control system. Figure (13a) shows the two set-point temperatures of the run, where steady-state oscillations were achieved to $\pm 1[^{\circ}C]$ of the set-point temperature. Figure (13b) shows the associated current vs time plot, where, when the set-point temperature changes from $1368[^{\circ}C]$ to $1369[^{\circ}C]$, the current maximizes to increase the vaporization of copper inside the vacuum chamber, which in turn raised the temperature to the new set-point. Further proof of temperature control can be found in Appendix A, where plots of temperature, current, and pressure vs time are shown.

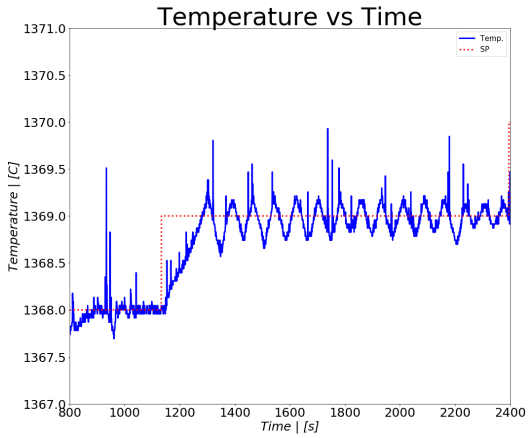


(a) Temperature vs time steady-state oscillation about set-point temperature during controlled deposition of copper (Cu).

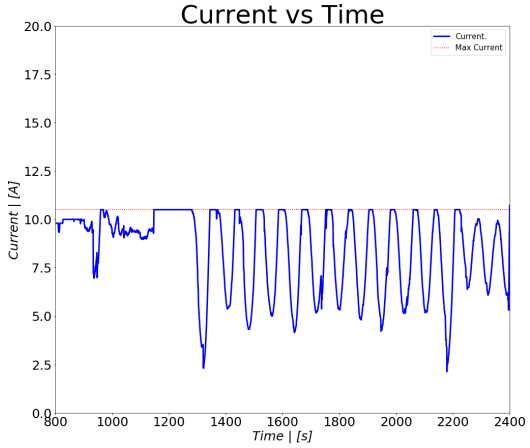


(b) Current vs time for the pressure-temperature control system during controlled deposition of copper (Cu).

Figure 13: Steady-state oscillation reached during a copper (Cu) deposition run.

The pressure-temperature model developed helped to form a basis of understanding for how an in-lab control system would function accurately. As for the control system, temperature control was achieved during steady state oscillations in the current and temperature. With temperature fluctuating around the set-point temperature of $\pm 1[^{\circ}C]$ shown in Figures (10), (13a), and, from Appendix A, (15a). From Figures (12a) and (12b), the difference between a controlled and uncontrolled deposition are shown. The pressure-temperature control system has been shown to achieve temperature control, and also provide a more uniform deposition of material when in use as compared to when not functioning or not in use.

* Chandler Fleuette: cjf1029@wildcats.unh.edu

[1] R. Darling, Microfabrication: Physical vapor deposition, EE-527 (2013).
[2] C. Alcock, V. Itkin, and M. Horrigan, Canadian Metallurgical Quarterly (1984).
[3] H.-P. Halvorsen, Control and simulation in labview (2017).
[4] N. Instruments, Pid theory explained (2011).

## Appendix A

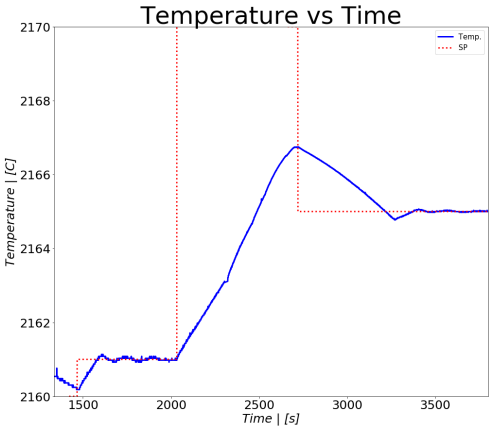


(a) Temperature vs time for the pressure-temperature control system achieving two different set-point steady-state oscillations in the same run.

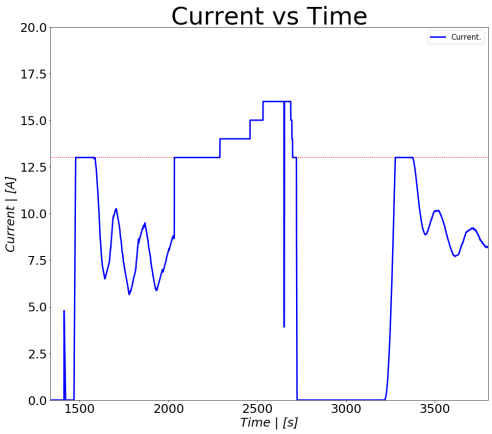


(b) Current vs time for the pressure-temperature control system achieving two different set-point steady-state oscillations in the same run.

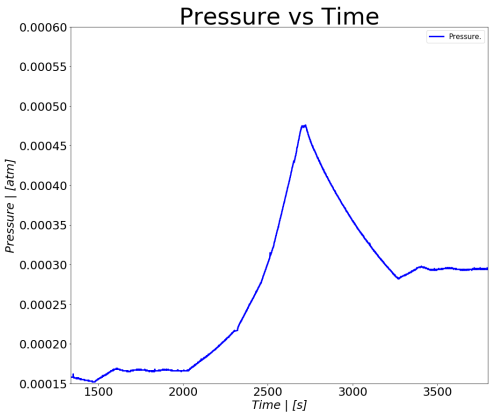


(c) Pressure vs time for the pressure-temperature control system achieving two different set-point steady-state oscillations in the same run.

Figure 14: Proof of temperature control.

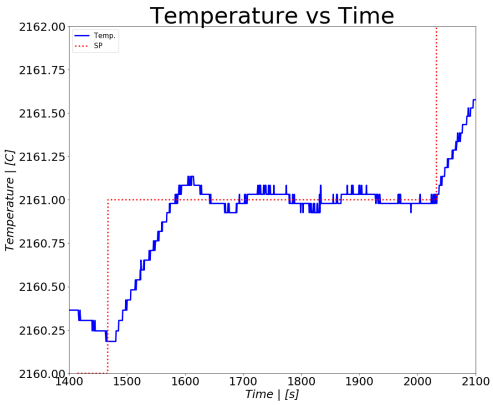


(a) Zoom of the temperature vs time for the pressure-temperature control system achieving set-point steady-state oscillation.

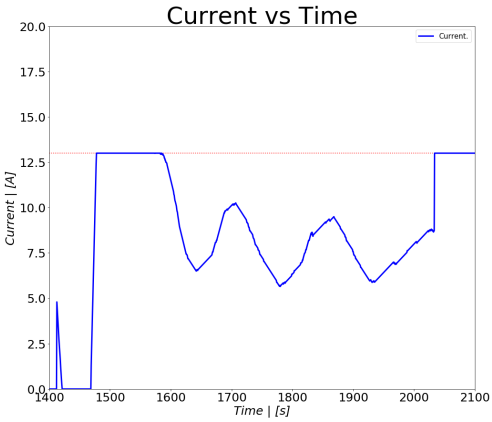


(b) Zoom of the current vs time for the pressure-temperature control system achieving set-point steady-state oscillation.

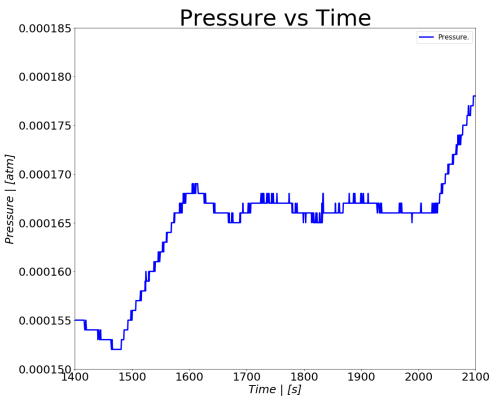


(c) Zoom of the pressure vs time for the pressure-temperature control system achieving set-point steady-state oscillation.

Figure 15: Zoom of low temperature, left side steady-state, from Figure (14) for proof of temperature control showing steady-state oscillation structure.